Int. J. Multiphase Flow, Vol. 7, pp. 191–210, 1981
Printed in Great Britain

0301-9322/81/020191-20$02.00/0
Pergamon/Elsevier

PRESSURE DISTRIBUTION IN BUBBLY FLOW THROUGH VENTURIS

N. T. THANG†
Darling Downs Institute of Advanced Education, Queensland, Australia

and

M. R. DAVIS
University of New South Wales, New South Wales, Australia

(*Received* 21 *May* 1979; *in revised form* 10 *August* 1980)

Abstract—The pressure distribution in vertical air–water mixture flows through venturis was investigated using area contraction ratios of 3.16 and 7.11 with variations in angles of convergence and divergence. The flow conditions were predominantly of the bubbly type and covered a range of gas volume fractions at the throat between 0.2 and 0.6. The one-dimensional momentum equation assuming isothermal flow with interphase relative motion was solved for the necessary relationship between pressure and area. An analysis was also developed to predict the pressure rise across a shock wave. Static pressure measurements obtained in eight venturi assemblies were compared with theoretical prediction and the results showed that the momentum equation assuming constant velocity ratio with properties normalized about the sonic throat pressure could account with fair accuracy for pressure in the converging passage of the venturis whilst downstream of the venturi throat the presence of a two-phase shock gave a good overall description of the steep pressure rise in supersonic flows. Departures from theory are accounted for in venturis with sharp contractions where three-dimensional flow effects gave rise to an appreciable transverse pressure gradient, a high velocity ratio and in some cases a vena contracta effect.

1. INTRODUCTION

Previous studies on two-phase flow through convergent–divergent nozzles were directed towards cases in which compressiblity effects of the mixture were predominant, such as the occurrence of critical flow to limit the discharge capacity. They dealt mainly with high quality droplet flows (Carofano & McManus 1969, Smith 1972). The study of lower quality two-component gas–liquid flow, namely bubble flow, through a venturi has received less attention in the literature. Further, a large number of flow models assumed an homogeneous structure in which the phases are uniformly distributed and move with the same velocity (Tangren *et al.* 1949, Campbell & Pitcher 1957). This facilitated the analysis but did not fully account for the actual dynamics of the flowing mixture. In the present work, the one-dimensional momentum equation in variable area flow is developed with allowance made for the relative velocity between the cocurrent phases. The theory is used to predict the pressure distribution along a number of venturi configurations. Like single-phase compressible flow, two-phase supersonic flow regions may exist in the diverging passage of a convergent–divergent nozzle, giving rise to a compression shock wave if the flow is suddenly decelerated. In recent years, this subject has been investigated by a number of authors (Witte 1969, Eddington 1970, Wijngaarden 1970, 1972) in which interphase relative motion was considered to be of significance in the shock wave characteristics. However, due to lack of experimental data, its effects have not been fully investigated. An analysis is given in this work to predict the pressure rise across a shock wave taking into account also the effect of relative velocity between the phases.

2. THEORETICAL CONSIDERATIONS

2.1 *Momentum equation*

The two-phase mixture is assumed to undergo changes of pressure and local void fraction from their initial values but there is no mass transfer between the two phases. The liquid phase is assumed to have a constant density ρ_L whilst the gas density ρ_G is related to the local

†Now at: Dept. of Mechanical Engineering, Monash University, Clayton, Victoria 3168, Australia.

pressure by a polytropic law with a compression index n. From other investigations (Davies 1967, Eddington 1970) the flow can be considered to be isothermal ($n = 1$). However, the polytropic relation will be retained in the discussion for generality.

The density of the gas phase is related to an initial reference condition denoted by a suffix zero by the equation

$$\rho_G = \rho_{G0}\left(\frac{p}{p_0}\right)^{1/n}$$

or [1]

$$\rho_G = \rho_{G0}\bar{p}^{1/n}.$$

The conservation of mass for each of the phases at two cross-sections of areas A_0 and A gives:

$$\alpha_0\rho_{G0}U_{G0}A_0 = \alpha\rho_G U_G A \quad [2]$$

and

$$(1-\alpha_0)\rho_L U_{L0}A_0 = (1-\alpha)\rho_L U_L A \quad [3]$$

where α is the void fraction, U_G and U_L are the cross sectional averages of gas and liquid phase velocities respectively. By introducing the velocity ratio

$$S = \frac{U_G}{U_L}, \quad [4]$$

[2] and [3] can be combined to give:

$$\frac{\alpha}{\alpha_0} = \frac{\bar{p}^{-(1/n)}}{\frac{S}{S_0}(1-\alpha_0) + \alpha_0\bar{p}^{-(1/n)}}. \quad [5]$$

It was shown by Davis (1971) that by ignoring interphase relative motion (i.e. $S = 1$) an expression for the local pressure as a function of area change could be obtained by direct integration of the momentum equation. In the following analysis it can be shown that if the velocity ratio, which in the general case is different from unity, remains constant then the basis relations proposed by Davis are still valid. However, if the velocity ratio is not constant, integration is possible only when suitable analytical expressions or empirical correlations are assumed for the variation of the velocity ratio (Thang 1976).

The momentum balance of the two-phase mixture can be simply written as

$$\alpha\rho_G U_G\frac{\mathrm{d}U_G}{\mathrm{d}x} + (1-\alpha)\rho_L U_L\frac{\mathrm{d}U_L}{\mathrm{d}x} = -\frac{\mathrm{d}p}{\mathrm{d}x}. \quad [6]$$

It is noted from [4] that

$$\frac{\mathrm{d}U_G}{\mathrm{d}x} = U_L\frac{\mathrm{d}S}{\mathrm{d}x} + S\frac{\mathrm{d}U_L}{\mathrm{d}x}. \quad [7]$$

Thus [6] can be arranged in the following form:

$$[(1-\alpha)\rho_L + \alpha\rho_G S^2]\,\mathrm{d}\left(\frac{1}{2}U_L^2\right) + U_L^2 S\alpha\rho_G\,\mathrm{d}S = -\mathrm{d}p. \quad [8]$$

If it is assumed that the velocity ratio is constant, [8] becomes

$$[(1-\alpha)\rho_L + \alpha\rho_G S^2]\,\mathrm{d}\left(\frac{1}{2}U_L^2\right) = -\,\mathrm{d}p\,. \qquad [9]$$

Substituting for α in [5], [9] can be written as

$$\left[\frac{(1-\alpha_0)\rho_L + \alpha_0\rho_{G0}S_0^2}{p_0}\right]\mathrm{d}\left(\frac{1}{2}U_L^2\right) = -(1-\alpha_0+\alpha_0\bar{p}^{-(1/n)})\,\mathrm{d}\bar{p}\,. \qquad [10]$$

By integrating both sides of [10], the following result is obtained:

$$\frac{\alpha_0\rho_{G0}S_0^2 + (1-\alpha_0)\rho_L}{2p_0}\quad (U_L^2 - U_{L0}^2) = (1-\alpha_0)(1-\bar{p}) - \frac{n\alpha_0}{n-1}(\bar{p}^{1-(1/n)} - 1)\,. \qquad [11]$$

From [2] and [4] the average liquid velocity is

$$U_L = U_{L0}\frac{S_0}{S}\frac{A_0}{A}\left[\frac{S}{S_0}(1-\alpha_0) + \alpha_0\bar{p}^{-(1/n)}\right]. \qquad [12]$$

Substituting for U_L in [11] with $S = S_0$

$$\frac{\alpha_0\rho_{G0}S_0^2 + (1-\alpha_0)\rho_L}{2p_0}\left[\left(\frac{A_0}{A}\right)^2(1-\alpha_0+\alpha_0\bar{p}^{-(1/n)})^2 - 1\right]U_{L0}^2 = (1-\alpha_0)(1-\bar{p}) - \frac{n\alpha_0}{n-1}(\bar{p}^{1-(1/n)} - 1)\,. \qquad [13]$$

By defining the dimensionless dynamic head factor D_0 as

$$D_0 = \frac{\alpha_0\rho_{G0}U_{G0}^2 + (1-\alpha_0)\rho_L U_{L0}^2}{p_0}, \qquad [14]$$

[13] becomes

$$\frac{D_0}{2}\left[\left(\frac{A_0}{A}\right)^2(1-\alpha_0+\alpha_0\bar{p}^{-(1/n)})^2 - 1\right] = (1-\alpha_0)(1-\bar{p}) - \frac{n\alpha_0}{n-1}(\bar{p}^{1-(1/n)} - 1)\,. \qquad [15]$$

Under isothermal condition where the compression index n is unity, the solution of the momentum equation can be found by integrating [10] to give

$$\frac{D_0}{2}\left[\left(\frac{A_0}{A}\right)^2(1-\alpha_0+\alpha_0\bar{p}^{-1})^2 - 1\right] = (1-\alpha_0)(1-\bar{p}) - \alpha_0\ln\bar{p}\,. \qquad [16]$$

Equations [15] and [16] give the necessary relationships between the local pressure ratio and the area ratio expressed in terms of known initial parameters α_0 and D_0. Further simplifications of [15] and [16] can be made by relating the flow properties to those at the sonic point instead of an arbitrary reference condition (Davis 1971). It is thus necessary at this point to derive an expression for the speed of sound in the mixture. In a compressible medium, the speed of sound wave propagation is given by the following insentropic relationship

$$a = \left(\frac{\partial p}{\partial \rho_m}\right)^{1/2}. \qquad [17]$$

The mixture density ρ_m is defined as

$$\rho_m = \alpha\rho_G + (1-\alpha)\rho_L . \qquad [18]$$

By combining [18] with [5]

$$\frac{\rho_m}{\rho_{m0}} = \frac{\mu + S}{\mu + S_0}\left[\frac{1}{\frac{S}{S_0}(1-\alpha_0) + \alpha_0\bar{p}^{-(1/n)}}\right] \qquad [19]$$

where μ is the mass flow ratio (m_G/m_L).

If S is a constant,

$$\frac{\rho_m}{\rho_{m0}} = \frac{1}{1-\alpha_0+\alpha_0\bar{p}^{-(1/n)}} . \qquad [20]$$

Thus, using [20] in [17]

$$a = \left(\frac{p_0}{\rho_{m0}}\right)^{1/2}\left(1-\alpha_0+\alpha_0\bar{p}^{-(1/n)}\right)\left(\frac{n\bar{p}^{1+(1/n)}}{\alpha_0}\right)^{1/2} . \qquad [21]$$

In general the speed of sound in an homogeneous two-phase mixture is

$$a = \left(\frac{np}{\alpha\rho_m}\right)^{1/2} \qquad [22]$$

which can be reduced to the familiar form

$$a = \left(\frac{\gamma p}{\rho}\right)^{1/2}$$

for a perfect gas when $\alpha = 1$ and $n = \gamma$.

It was noted that the dimensionless dynamic head factor D which was defined previously as

$$D = \frac{\alpha\rho_G U_G^2 + (1-\alpha)\rho_L U_L^2}{p} \qquad [23]$$

would include the special case where the velocity ratio is unity. In this particular case, the mean mixture velocity U_m is identical with both phase velocities U_G and U_L thus giving

$$D_H = \frac{\rho_m U_m^2}{p} . \qquad [24]$$

It is proposed that by equating [23] and [24], a definition of the mixture velocity in the general case of flow with interphase relative motion may be made as follows:

$$U_{mD} = \left[\frac{\alpha\rho_G U_G^2 + (1-\alpha)\rho_L U_L^2}{\rho_m}\right]^{1/2} \qquad [25]$$

or

$$U_{mD} = \left(\frac{Dp}{\rho_m}\right)^{1/2} . \qquad [26]$$

The Mach number can now be defined as the ratio of the mixture velocity U_{mD} to the velocity of sound "a" thus

$$M = \left(\frac{\alpha D}{n}\right)^{1/2}. \qquad [27]$$

The question of defining a suitable Mach number for two-phase flow with interphase relative velocity has not been clearly resolved in the literature. This has caused ambiguity in such terms as subsonic and supersonic flows in some areas of two-phase flow, particularly in nozzle flows. It is clearly recognizable that in an homogeneous flow with no relative phase velocity a definition of Mach number based on an average mixture velocity will produce a Mach number of unity at the throat of a nozzle under critical flow situations. This can be seen as a logical extension of the criterion for flow choking in compressible single-phase flow. However, this same result cannot be obtained in two-phase flows with interphase relative motion if one maintains a definition of average mixture velocity based on a mass or volume flow rate basis. The definition of Mach number given by [27] is proposed to simplify the problem and to give a Mach number of unity at the throat of the venturi in two-phase flow with constant velocity ratio. This can be demonstrated by using [16] with the properties related to those at the throat (instead of those at the initial state) where the condition $(dA/dp) = 0$ holds, which leads to $M^* = 1$ (*denotes sonic point condition).

A simple relationship is now derived for the Mach number calculated for a flow with no relative velocity and the velocity ratio that would be present in the proposed constant velocity ratio model to make M equal to unity at the throat in critical flow condition. By defining the gas volume fraction β as

$$\beta = \frac{Q_G}{Q_G + Q_L} \qquad [28]$$

where Q_G and Q_L are the gas and liquid volume flow rates respectively, it can be shown that for flow with no relative velocity,

$$M_{NS}^2 = \frac{\beta}{1-\beta}\frac{1+\mu S}{p}\frac{\rho_L Q_L^2}{A^2}. \qquad [29]$$

With constant velocity ratio assumption, the following relation is obtained:

$$M_{CS}^2 = \frac{\beta}{1-\beta}\frac{1+\mu S}{S}\frac{\rho_L Q_L^2}{A^2 p}. \qquad [30]$$

Thus

$$\left(\frac{M_{CS}}{M_{NS}}\right)^2 = \frac{1+\mu S}{S(1+\mu)} \qquad [31]$$

or since

$$\frac{1+\mu S}{1+\mu} \simeq 1,$$

$$\left(\frac{M_{CS}}{M_{NS}}\right)^2 = \frac{1}{S}. \qquad [32]$$

At the sonic throat in the model for flow with constant velocity ratio, the Mach number M_{CS} is equal to unity, the velocity ratio would thus assume the following value

$$S = M^*_{NS}{}^2. \tag{33}$$

This relation can be used to determine the velocity ratio in a choked flow under the constant velocity ratio assumption. It is obvious that if S is greater than unity, the above equation implies that M^*_{NS} is also greater than unity.

From [27] if one assumes $n = 1$ then at the sonic condition (denoted by *) the following simple relation can be obtained

$$D^* = \frac{1}{\alpha^*}. \tag{34}$$

Thus, the solution of the momentum equation [16] can be written as

$$\frac{A^*}{A} = \frac{\{1 + 2\alpha^*[(1-\alpha^*)(1-\bar{p}^*) - \alpha^* \ln \bar{p}^*]\}^{1/2}}{1 - \alpha^* + \alpha^* \bar{p}^{*-1}} \tag{35}$$

where properties are now referred to those at the sonic throat. Variation of the dimensionless pressure in terms of the throat area ratio is seen to be characterized by a single parameter, namely the sonic point void fraction α^*.

2.2 *Compression shock wave*

As in single-phase compressible flow, the occurrence of a compression shock wave involves supersonic flow such as that in the diverging section of a venturi. The following analysis derives an expression for the pressure ratio on two sides of a shock with a view to determining whether two-phase shock wave did exist in the flow down-stream of a venturi contraction in this work.

State 1 refers to conditions immediately upstream of a shock wave in a gas–liquid mixture whilst state 2 immediately follows the shock. The shock thickness is assumed to be small compared to the diameter of the flow channel so that the cross-sectional areas A_1 and A_2 can be considered equal. One also makes the usual assumptions that the mixture behaves isothermally and the thermal energy equation can thus be ignored.

A force balance across the shock can be written as

$$\alpha_1 \rho_{G1} U^2_{G1} + (1-\alpha_1)\rho_L U^2_{L1} + p_1 = \alpha_2 \rho_{G2} U^2_{G2} + (1-\alpha_2)\rho_L U^2_{L2} + p_2 \tag{36}$$

which can be arranged in the following form

$$\frac{p_2}{p_1} = (1 + D_1)/\left[1 + \frac{\alpha_2 \rho_{G2} U^2_{G2} + (1-\alpha_2)\rho_L U^2_{L2}}{p_2}\right] \tag{37}$$

where

$$D_1 = \frac{\alpha_1 \rho_{G1} U^2_{G1} + (1-\alpha_1)\rho_L U^2_{L1}}{p_1}.$$

Continuity requirement for the two phases gives

$$\alpha_1 \rho_{G1} U_{G1} = \alpha_2 \rho_{G2} U_{G2} \tag{38}$$

$$(1-\alpha_1) U_{L1} = (1-\alpha_2) U_{L2}. \tag{39}$$

By combining [38] and [39] in [37] one obtains a quadratic equation in (p_2/p_1), the pressure ratio across the shock

$$\left(\frac{p_2}{p_1}\right)^2 - \left[1 + D_1 - D_1(1-\alpha_1) \quad \frac{\mu S_2 + 1}{\mu S_1 + 1}\right]\left(\frac{p_2}{p_1}\right) + \alpha_1 D_1 \frac{S_1}{S_2}\frac{\mu S_2 + 1}{\mu S_1 + 1} = 0. \qquad [40]$$

2.2.1 *Constant velocity ratio across the shock.* Since $S_1 = S_2$ the velocity ratio terms disappear from [40] and this becomes

$$\left(\frac{p_2}{p_1}\right)^2 - (1 + \alpha_1 D_1)\frac{p_2}{p_1} + \alpha_1 D_1 = 0. \qquad [41]$$

The non-trivial solution to the above equation is

$$\frac{p_2}{p_1} = \alpha_1 D_1 \qquad [42]$$

or from [27]

$$\frac{p_2}{p_1} = M_1^2. \qquad [43]$$

The above result is consistent with that derived by Campbell & Pitcher (1975) in the special case where the velocity ratio is unity throughout the flow. To calculate the Mach number at state 2 after the shock, the void fraction and the dynamic head factor can be related to those in front of the shock by the following relations

$$\alpha_2 = 1/[1 + (1-\alpha_1)D_1] \qquad [44]$$

$$D_2 = [1 + (1-\alpha_1)D_1]/\alpha_1 D_1. \qquad [45]$$

Hence

$$\alpha_2 D_2 = 1/\alpha_1 D_1 \qquad [46]$$

which shows that

$$M_2 = \frac{1}{M_1}. \qquad [47]$$

This result was also obtained by Eddington (1970) but for the more restricted condition of $S_2 = S_1 = 1$.

2.2.2 *Different velocity ratios across the shock.* Note that this case does not impose any condition on the nature of the velocity ratio on two sides of the shock. The velocity ratio may be a variable or may remain constant upstream and downstream of the shock, but its local values at states 1 and 2 are assumed to be different due to the presence of the shock as a finite flow discontinuity.

The solution to [40] gives:

$$\frac{p_2}{p_1} = \frac{1}{2}\left\{1 + D_1 - (1-\alpha_1)D_1\frac{\mu S_2 + 1}{\mu S_1 + 1} + \sqrt{\left(\left[(1 + D_1) - (1-\alpha_1)D_1\frac{\mu S_2 + 1}{\mu S_1 + 1}\right]^2 - 4\alpha_1 D_1 \frac{S_1}{S_2}\frac{\mu S_2 + 1}{\mu S_1 + 1}\right)}\right\}. \qquad [48]$$

If μ is ignored,

$$\frac{p_2}{p_1} = \frac{1}{2}\left[1 + \alpha_1 D_1 + \sqrt{\left((1+\alpha_1 D_1)^2 - 4\alpha_1 D_1 \frac{S_1}{S_2}\right)}\right]. \qquad [49]$$

The positive root is selected to ensure that $(p_2/p_1) = \alpha_1 D_1$ at $S_2/S_1 = 1$ for cases where $\alpha_1 D_1 > 1$ (i.e. supersonic flow upstream of the shock). The negative root gives $(p_2/p_1) = 1$ (trivial solution) in this case and gives $(p_2/p_1) < 1$ for $(S_2/S_1) > 1$, which is clearly physically unrealistic.

Figure 1 specifies the regions of possible solution for [49]. For the case $(S_2/S_1) > 1$, the region of possible solution is defined by the following upper and lower bounds which correspond to the case where $(S_2/S_1) \to \infty$ and $(S_2/S_1) = 1$ respectively:

$$\left(\frac{p_2}{p_1}\right)_{1\max} = 1 + \alpha_1 D_1$$

$$\left(\frac{p_2}{p_1}\right)_{1\min} = \alpha_1 D_1 .$$

The other case where $(S_2/S_1) < 1$ is normally expected to occur as there is tendency for the less dense gas phase to slip in the region preceding a shock due to a strong expansion there. However, in the subsonic flow following the shock, the mixture will decelerate considerably with a possible change in the bubble structure and the relative motion of the gas phase with respect to the liquid phase can be considered quite small. The upper bound of the pressure ratio is

$$\left(\frac{p_2}{p_1}\right)_{2\max} = \alpha_1 D_1 .$$

The lower bound of the pressure ratio corresponds to the smallest value of (S_2/S_1) for which the quantity in the square root of [49] does not become negative,

$$\frac{S_2}{S_1} = \frac{4\alpha_1 D_1}{(1+\alpha_1 D_1)^2} . \qquad [50]$$

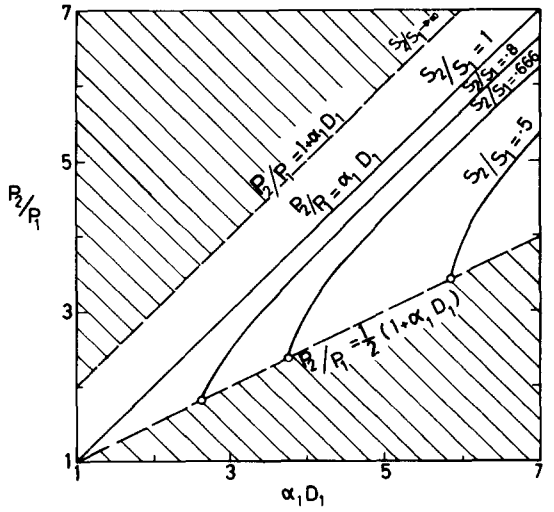

Figure 1. Pressure rise across a shock wave.

In this case,

$$\left(\frac{p_2}{p_1}\right)_{2\min} = \frac{1}{2}(1+\alpha_1 D_1). \qquad [51]$$

Using [51] it can be shown that

$$\alpha_2 D_2 = \frac{4\alpha_1 D_1}{(1+\alpha_1 D_1)^2} \cdot \frac{S_1}{S_2}$$

or from [50]

$$\alpha_2 D_2 = 1. \qquad [52]$$

Thus the line representing the lower bound for the pressure ratio also represents the condition for which $\alpha_2 D_2 = 1$. If it is assumed that S_2 remains constant after the shock the above equation shows that $M_2 = 1$. Any point lying below this line in figure 1 would result in $M_2 > 1$ and this has been shown by Witte (1969) for example to be impossible for a shock.

In summary, since it is generally expected that when interphase relative motion is present in the flow it will be greater upstream of the shock than downstream, the results of figure 1 show that for flows with the same Mach number at the shock, an effect of this decrease in the velocity ratio across the shock is to reduce the pressure ratio compared with the case when S remains constant.

3. EXPERIMENTAL EQUIPMENT

The test venturis were bored out of Perspex cylindrical blocks. Each venturi assembly consists of three parts: the conical convergent channel, the cylindrical throat and the conical divergent channel. A total of eight venturi assemblies were used. The relevant geometrical features are given in table 1. The area contraction ratio for four venturis of series A is 3.16 and that for four venturis of series B is 7.11.

Table 1. Geometric details for venturi configurations

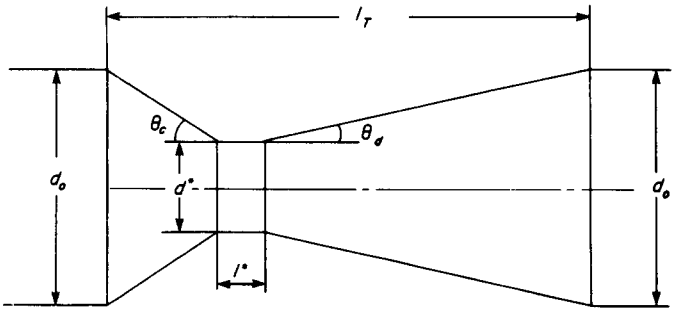

Venturi	d^* (mm)	d_0 (mm)	ℓ^* (mm)	ℓ_T (mm)	θ_c (°)	θ_d (°)	A_0/A^*
A1	28.57	50.8	14.29	147.64	14.04	7.12	3.16
A2	28.57	50.8	14.29	103.19	14.04	14.04	3.16
A3	28.57	50.8	14.29	114.30	45	7.12	3.16
A4	28.57	50.8	14.29	69.85	45	14.04	3.16
B1	19.05	50.8	5.92	200.02	14.04	7.12	7.11
B2	19.05	50.8	5.92	136.52	14.04	14.04	7.11
B3	19.05	50.8	5.92	152.40	45	7.12	7.11
B4	19.05	50.8	5.92	88.90	45	14.04	7.11

Measured air and water flow rates were fed separately into a multi-jet nozzle assembly where they were mixed in a contracting cone by turbulence generated by the jets. Under most conditions observed in this investigation a fairly uniform mixture was produced (Thang & Davis 1979). The mixture was introduced into a vertical clear Perspex pipe of 50.8 mm i.d. upstream of the venturi. This settling length is 25 diameters long. On leaving the venturi, the flow passed through an additional main pipe 12 diameters long and was discharged through a return bend to the laboratory main sump.

Static pressure was measured through small wall tappings by a calibrated mercury manometer for vacuum and gauge pressure up to approx. 200 kPa and by a standard precision gauge for higher pressure. Pressure fluctuations in flows approaching slugging conditions, especially at the throat and diverging channel caused variations in pressure readings of up to 3 per cent.

4. INTERPRETATION OF PRESSURE MEASUREMENTS

4.1 *Pressure distribution across venturi*

Pressure measured along the venturis in 9 flow conditions (table 2) can be normalized on inlet as well as throat conditions to compare with prediction from theory. Inlet normalization is used for both subsonic and supersonic flows whilst throat normalization is used for flows which became sonic at the throat.

4.1.1 *Normalization on inlet conditions.* Equation [16] applies to the general case of flows having a constant velocity ratio, although the latter is initially assumed to be unity in evaluating α_0 and D_0 for each flow condition. Figure 2 shows typical results for venturi A1 (larger throat) and B1 (smaller throat). For flow conditions 1–5 in A1 and 1, 2 for B1 the Mach number calculated from wall pressure is less than unity at the geometric throat and as a result, the prediction of pressure variation in the divergent passage for supersonic flows by the lower halves of the theoretical curves is not applicable to these flows.

In general, there is moderate agreement between theory and experiment in the converging passage. The pressure of the flow immediately before the throat is higher than predicted whilst the opposite is true for the pressure at the throat itself. This is due to three-dimensional flow effects caused by the sharp angle of the converging passage. These effects are most noticeable in the results of venturis which have a short converging channel and a large inlet angle of 90°.

Table 2. Typical flow condition data. β^*: Gas volume fraction at the throat

Venturi	Flow Condition	$m_G \times 10^3$ (kg/s)	m_L (kg/s)	P_{inlet} (KPa)	β^*	U_m^* (m/s)
A1	1	1.49	4.131	127.1	0.236	8.45
	2	2.78	4.131	132.07	0.364	10.14
	3	4.07	4.131	136.6	0.455	11.84
	4	2.36	7.156	164.7	0.272	15.34
	5	5.92	7.156	201.6	0.437	19.84
	6	11.36	7.156	235.9	0.545	24.54
	7	3.63	10.120	258.7	0.282	22.00
	8	11.04	10.120	348.6	0.415	27.01
	9	22.97	10.120	441.9	0.506	31.97
B1	1	1.00	2.921	153.6	0.280	14.26
	2	2.24	2.921	179.5	0.418	17.63
	3	4.04	2.921	201.8	0.544	22.54
	4	1.48	4.131	231.3	0.292	20.52
	5	2.76	4.131	274.3	0.358	22.60
	6	5.54	4.131	333.1	0.448	26.32
	7	5.92	4.771	401.4	0.403	28.08
	8	11.71	4.771	500.6	0.491	32.92
	9	19.53	4.771	602.9	0.554	37.54

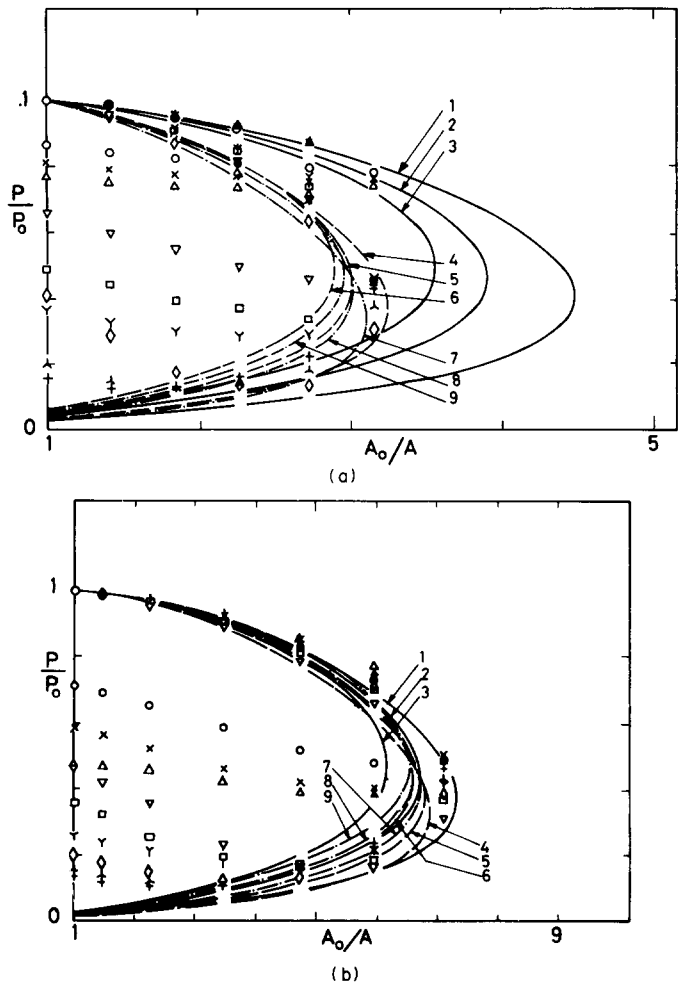

Figure 2. Pressure variation normalized on inlet conditions:

(a) Venturi A1			(b) Venturi B1		
	Flow	α_0		Flow	α_0
○	1	0.194	○	1	0.159
×	2	0.302	×	2	0.267
△	3	0.380	△	3	0.369
▽	4	0.145	▽	4	0.115
□	5	0.257	□	5	0.171
Y	6	0.355	Y	6	0.254
◇	7	0.105	◇	7	0.208
Y	8	0.209	Y	8	0.294
+	9	0.303	+	9	0.366

The flow near the wall in following the large directional change presented by the inlet wall produces a pressure gradient in the transverse direction. The presence of the radial pressure gradient will cause the pressure measured at the wall to be higher than at the centre of the flow. By similar reasoning at the throat, as the flow streamlines change their curvature due to the sharp convex corner at the throat inlet, pressure at the wall will be lower than in the central part of the flow. The net result gives a much higher pressure gradient than that would have been predicted by one-dimensional theory assuming uniform pressure across the flow section. In the divergent passage, the poor pressure recovery was caused by the occurrence of flow separation. For flows with the same water flow rates, increasing the air flow rates aggravates flow separation after the throat and causes greater losses.

In other flow conditions not mentioned above, theory predicts a Mach number in excess of unity at the throat and in the divergent passage. Thus the flows are expected to follow the part of the curve predicted in the divergent channel for supersonic flows. However, it appears that there is not sufficient overall pressure differential for most flows to sustain supersonic flow. As a result, pressure starts to rise early in the divergent passage which in compressible flow will give rise to a shock. In the work by Muir & Eichhorn (1963, 1967) who reported shock wave in a convergent–divergent nozzle, isothermal flow theory also predicted lower pressure than experimental values in the divergent passage for their flow conditions with throat void fractions between 0.10 and 0.33. In the present work, it was not possible to directly observe any shock wave in the divergent passage or in the constant area tailpipe. However, the high pressure rise observed in these supersonic flows will be discussed in section 4.2.

From figure 2 it is also seen that theory predicts a larger throat size than the true throat for a number of flow cases, especially for flows in the higher range of void fraction α^* in venturis A1 and B1. The existence of interphase relative motion in the actual flow situation may be partly responsible for the above discrepancy between the one-dimensional theory and experimental results. In a flow having relative velocity, the void fraction α_0 will be less than the gas volume fraction β_0 if the velocity ratio S exceeds unity. As a result, the flow will generally need to accelerate further to reach sonic condition than in the case without relative motion. Given a fixed initial pressure p_0, this may be accomplished by either a more rapid pressure drop or by a smaller throat size. Since the pressure gradient along the convergent channel is used mainly to accelerate the liquid phase which makes up the bulk of the mass of the mixture, the pressure gradient required will be less in the case of flow with relative velocity because the velocity of the liquid phase is reduced in this case. To satisfy momentum conservation, it is thus not possible to have a larger pressure gradient in flows with $S > 1$. It would then be reasonable to expect that the flow will need a smaller throat to accelerate to critical conditions. This then provides the necessary correction on the predicted throat area and brings it closer to the actual value. Figure 3 illustrates the effect of relative velocity on the prediction of the sonic throat size for one supersonic flow condition of venturis A1 and B1. The agreement between predicted and real throat area improves with increases in the velocity ratio. In figure 3, it is also possible to observe the decrease in the pressure gradient along the flow as the velocity ratio assumes higher values for a fixed venturi geometry. Void probe measurements (Thang & Davis 1979) have shown that the velocity ratios at the throat of venturis A1 and B1 are greater than unity (between 1.05 and 1.30) and the curves of figure 3 demonstrate that the effect of velocity ratio on pressure distribution is in general agreement with the previous observations of velocity ratio under similar flow conditions. It is thus clear that the existence of phase relative motion with $S > 1$ can to a certain extent reconcile the discrepancies between one-dimensional theory and experimental observations. This point will be discussed more fully using the actual velocity ratios obtained from void probe measurements in section 4.1.2.

Static pressure probes were used to check the pressure at the centre line of the venturi contraction to determine the extent of three-dimensional flow effects. The measurements in venturis of both throat sizes showed that in all cases the pressure at the centreline is higher than at the wall. The difference is particularly high for venturis with a large convergence angle. This is expected as the wall suction effect of the liquid phase will be more severe for sharper inlet passages as was shown in the earlier void probe study (Thang & Davis 1979). However, as the gas content of the mixture is increased, the effect of suction becomes less pronounced and the transverse pressure gradient is smaller. The results as shown in table 3 illustrate these trends. Figure 4 compares theory and experiment using the wall pressure p_w^* and the centreline pressure p_c^* in two separate cases. The predicted dimensionless throat pressure $(p^*/p_0)_{PRE}$ which is obtained from [16] is in closer agreement with experimental results when the centreline throat pressure is used.

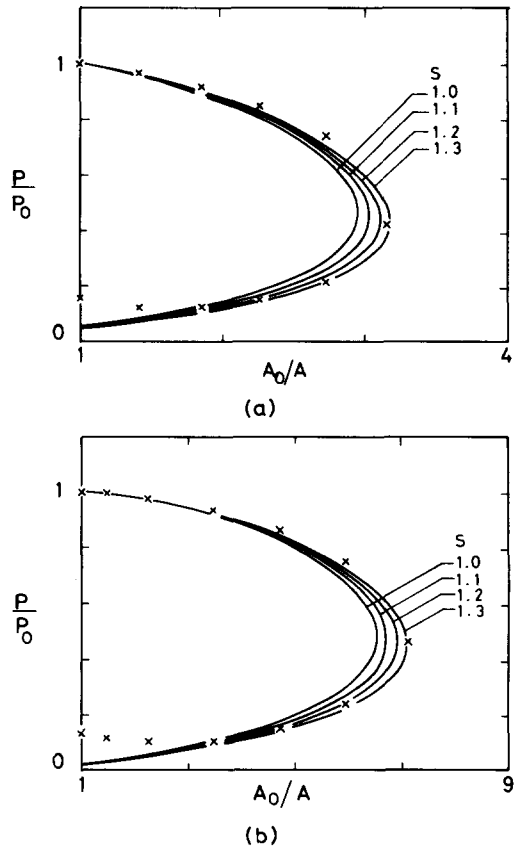

Figure 3. Effect of non-unity velocity ratio on pressure variation: (a) venturi A1, (b) venturi B1.

4.1.2 *Normalization on sonic throat conditions.* From [38] the pressure variation with respect to area change is characterized by the void fraction at the sonic throat α^* which in turn is dependent upon the velocity ratio and the gas volume fraction at the throat. The velocity ratio is assumed to be constant and its value predicted by [36]. These values are compared with those measured from a void probe at the venturi throat (Thang & Davis 1979) for a number of

Table 3. Comparison of pressure measured at the wall and centre line of the throat in two venturis

Venturi	Flow Condition	β_0	$\frac{p_w^*}{p_0}$	$\frac{p_c^*}{p_0}$	$\left(\frac{p_c^* - p_w^*}{p_c^*}\right)\%$
A1	1	0.194	0.779	0.786	0.9
	2	0.302	0.755	0.767	1.6
	3	0.380	0.735	0.750	2.0
	4	0.145	0.454	0.487	6.8
	5	0.275	0.447	0.482	7.3
	6	0.355	0.460	0.496	7.2
	7	0.105	0.300	0.339	12.2
	8	0.209	0.374	0.409	8.5
	9	0.303	0.425	0.461	7.8
A4	1	0.180	0.686	0.753	8.9
	2	0.287	0.662	0.735	9.9
	3	0.349	0.647	0.722	10.4
	4	0.123	0.327	0.476	31.3
	5	0.235	0.330	0.468	29.5
	6	0.334	0.380	0.490	22.4
	7	0.091	0.118	0.339	65.2
	8	0.190	0.241	0.407	40.8
	9	0.282	0.323	0.451	28.4

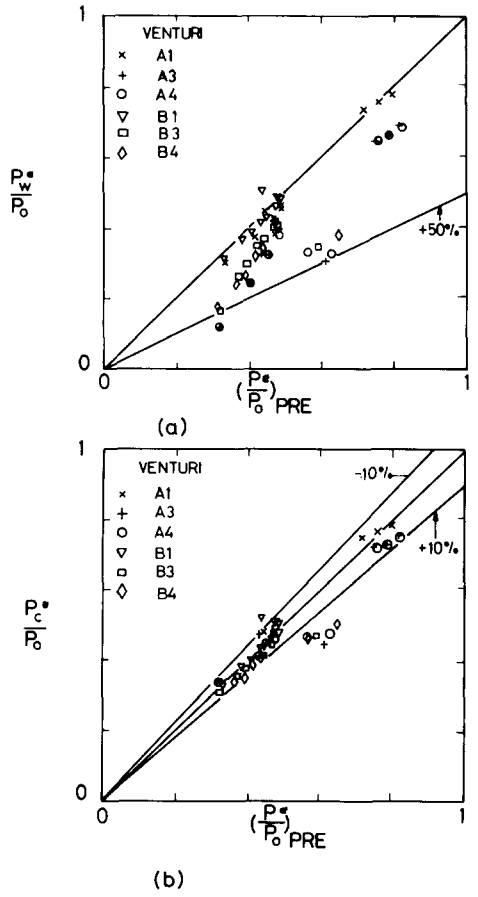

Figure 4. Comparison between experimental and predicted throat pressure assuming unity velocity ratio: (a) wall position, (b) centre-line position.

flow conditions. Although the velocity ratio data is limited, the trends in velocity ratio for flows ranging in mean throat void fraction between 0.14 and 0.47 and gas velocity between 9 and 33 m/s may be considered broadly representative of other flow conditions in the same venturi geometry. Table 4 summarizes the available velocity ratios measured at the throat of four venturis. The normalized results using the centreline throat are presented in figures 5(a) and 5(b). The corresponding velocity ratios calculated from [36] are also given for all the applicable flow conditions in these two figures. It is seen that these values are fairly close to unity but compare favourably with void probe results in table 4, the discrepancy becoming more noticeable in venturis with a large inlet angle (A4 and B4). Figure 6 compares the experimental inlet pressure normalized about the throat value (p_0/p_c^*) with that predicted by the model using

Table 4. Velocity ratio values from void probe measurements at the throat of four venturis

	FLOW CONDITION					
Venturi	1	3	4	6	7	9
A1	1.09	1.01	1.12	1.09	1.09	1.03
A4	1.57	1.41	1.49	1.35		
B1	1.28	1.04	1.27	1.18		
B4	1.52	1.49	1.47	1.58		

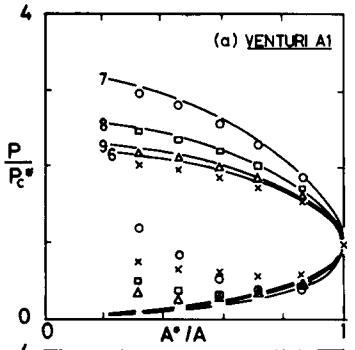

SYMBOL	FLOW	A1 S	A1 α*	A3 S	A3 α*	A4 S	A4 α*
×	6	1.13	0.494				
o	7	1.00	0.257	SUBSONIC		SUBSONIC	
□	8	1.13	0.364				
△	9	1.16	0.449	1.01	0.465	1.00	0.466

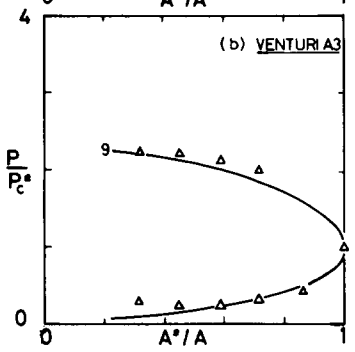

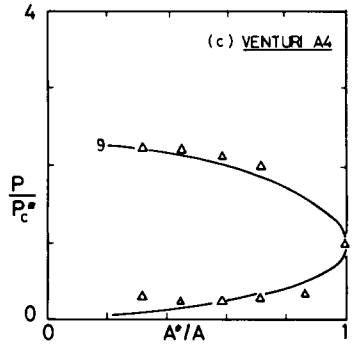

(a)

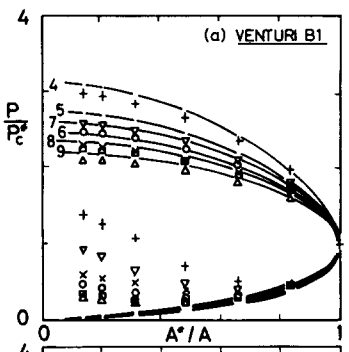

SYMBOL	FLOW	B1 S	B1 α*	B3 S	B3 α*	B4 S	B4 α*
+	4	1.05	0.270	SUBSONIC		SUBSONIC	
▽	5	1.06	0.335	1.00	0.341	1.03	0.338
×	6	1.12	0.409	1.07	0.414	1.13	0.407
o	7	1.12	0.367	1.05	0.373	1.19	0.358
□	8	1.18	0.443	1.14	0.447	1.14	0.445
△	9	1.15	0.509	1.14	0.499	1.19	0.512

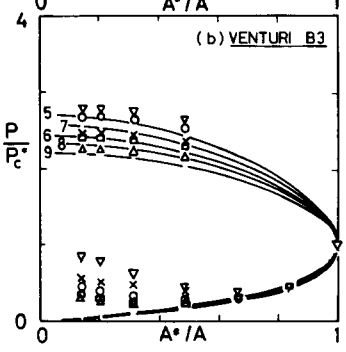

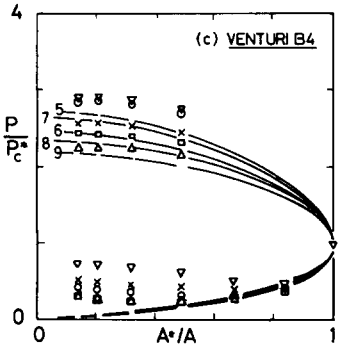

(b)

Figure 5. Pressure variation normalized on sonic throat conditions: (a) series A, (b) series B.

a constant velocity ratio (given in figures 5a and 5b). Since p_0 is least influenced by three-dimensional flow effects, experimental results agree with the predicted values to within 9.6 per cent although most data points fit well within a ±5 per cent scatter band.

In venturis A1, A2 and B1, B2 with a more gradual inlet angle, the discrepancy between theory and experiment may be caused by normalizing about a rather high pressure at the throat.

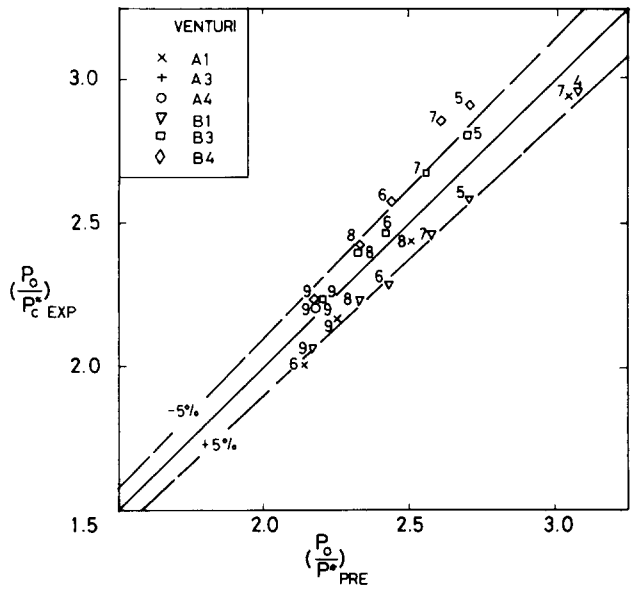

Figure 6. Comparison between predicted and experimental inlet pressure using constant velocity ratio model (numbers indicate flow conditions).

The pressure is now normalized about the throat wall value and the results for venturis B1 and B2 are shown in figure 7(a) and better overall agreement is observed. It can thus be concluded that in venturis with a gradual rate of area contraction, normalization about the wall throat pressure gives acceptable agreement with one-dimensional constant velocity ratio theory and small discrepancies could be due to variation of pressure across the section.

In venturis B3 and B4 which have an identical convergent section and inlet angle of 90°, normalization about centreline throat pressure still gives higher pressure ratios than predicted in the convergent passage (figure 5b). Using the constant velocity ratio model, the higher pressure profiles as shown by the experimental data entail a smaller void fraction at the throat than predicted. For the same measured throat pressure, this requires a higher velocity ratio as also suggested by the experimental void probe values at the throat (table 4). From [33] a higher velocity ratio means that the Mach number M^*_{NS} will increase and this can be achieved by a higher mixture velocity at the throat for the same pressure and mass flow rates. The latter suggests that the flows in venturis B3 and B4 may exhibit a vena contracta which reduces the cross-sectional flow area at the throat. Void probe measurement in flow conditions 1 and 4 of venturi B4 at the throat has confirmed the presence of a vena contracta (Thang & Davis 1979).

A qualitative estimate of the effect of a vena contracta on the pressure profile can be obtained by assuming a smaller flow cross section. On the basis of the void probe data, it is assumed that a reduction of 10 per cent in the area occurs in all flow conditions of venturis B3 and B4 and pressure normalization is made about the new throat condition. The results are shown in figure 7(b) and better agreement in the convergent passage is observed. The predicted velocity ratios in these cases (between 1.23 and 1.47) are not excessive compared with the measured velocity ratios in venturi B4 between 1.47 and 1.58 (table 4). However, vena contracta may not be the only effect which accounts for the high pressure profiles in venturis B3 and B4. Appreciable frictional losses in the sharp contraction of these venturis may give rise to a higher pressure drop than predicted assuming no energy dissipation. Except for a narrow region immediately after the throat, one dimensional theory does not predict favourably the pressure distribution in the divergent passage of all venturis (figures 5a and 5b) and none of the corrections for velocity ratio, transverse pressure gradient or vena contracta effects will resolve the discrepancies in the divergent passage.

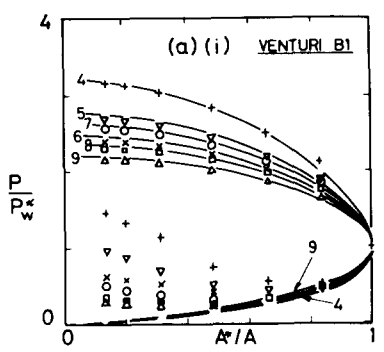

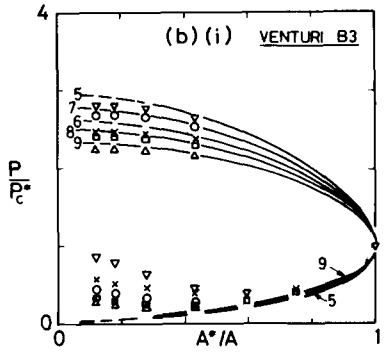

7(a)(i)

Flow Cond.		S	α^*
+	4	1.19	0.257
▽	5	1.16	0.325
×	6	1.23	0.398
○	7	1.22	0.357
□	8	1.25	0.435
△	9	1.24	0.499

7(b)(i)

Flow Cond.		S	α^*
▽	5	1.23	0.295
×	6	1.32	0.364
○	7	1.29	0.325
□	8	1.41	0.395
△	9	1.41	0.447

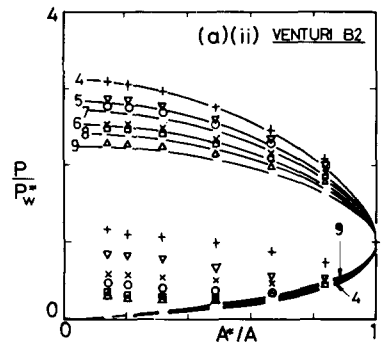

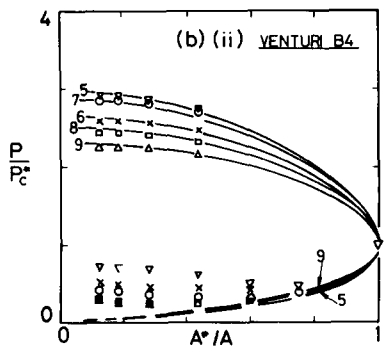

7(a)(ii)

Flow Cond.		S	α^*
+	4	1.06	0.268
▽	5	1.28	0.313
×	6	1.28	0.382
○	7	1.43	0.336
□	8	1.44	0.416
△	9	1.44	0.479

7(b)(ii)

Flow Cond.		S	α^*
▽	5	1.26	0.292
×	6	1.39	0.357
○	7	1.47	0.311
□	8	1.41	0.394
△	9	1.47	0.459

Figure 7. Normalization on throat pressure: (a) measured at the wall, (b) measured on centre-line with effect of a vena contracta.

4.2 *Pressure rise downstream of venturis*

Figure 8 shows typical pressure distribution downstream of the venturi throat in venturis A1 and B1. In venturis having identical diffusers, increases in the gas volume fraction and/or mass flux at the throat resulted in longer recovery distance in the tailpipe. Venturis with larger divergence angles generally resulted somewhat unexpectedly in more pressure rise in the tailpipe and longer recovery distance for same flow conditions. These results agreed with those

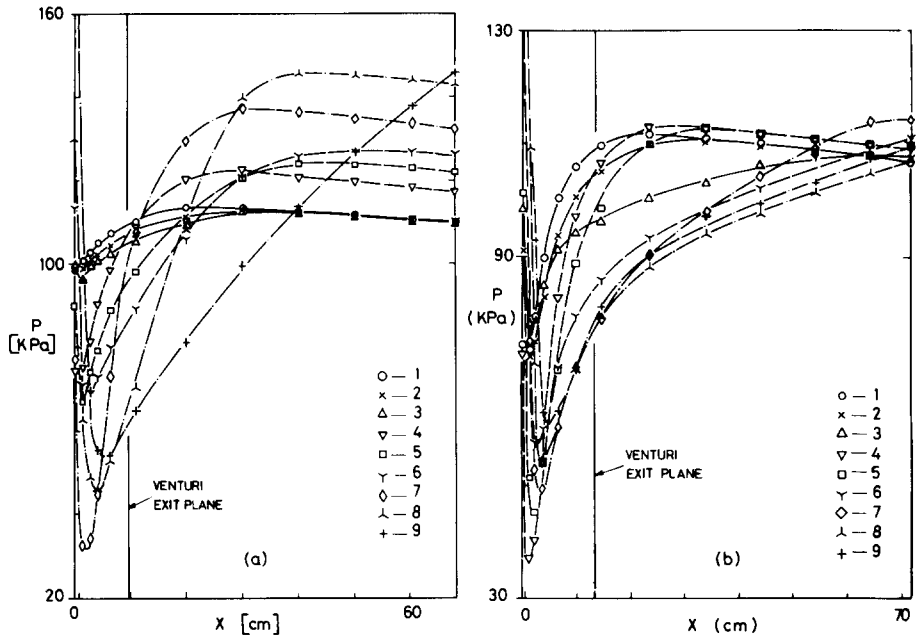

Figure 8. Pressure rise downstream of venturi throat: (a) venturi A1, (b) venturi B1 (numbers indicate flow conditions).

of Hench & Johnston (1972) in different diffuser geometry and flow parameters from the present work.

In all supersonic flow conditions investigated in the previous section, a strong pressure rise was recorded in the divergent section of the venturis and might continue for a considerable distance in the tailpipe before a peak is reached. Since the flow was supersonic at the point where minimum pressure occurs and subsonic at the peak of the pressure rise profile, the pressure rise observed might suggest that a phenomenon similar to a two-phase shock may be present. By denoting p_1 the minimum pressure and p_2 the maximum pressure further downstream, the ratio (p_2/p_1) can be compared with theoretically predicted values for a shock. Figure 9(a) compares these respective values assuming unity velocity ratio. Those data points representing conditions where Mach numbers were not substantially greater than unity showed closer agreement with theory. A more realistic comparison was made in figure 9(b) where best estimates for the velocity ratio obtained from void probe measurements (Thang & Davis 1979) were used in predicting the pressure rise. The better agreement observed here indicates that phase relative velocity has a significant effect on the pressure ratio across a shock.

The shock wave analysis in section 2.2 does not take into account the effect of area change whilst in practice the flow paths between p_1 and p_2 produces an increase in area. However, the flow was observed to separate from the wall in the divergent passage (Thang & Davis 1979) and it is not therefore expected that the pressure rise component due to subsonic diffusion following the shock would be realized. This was confirmed by calculations on the overall pressure rise including an ideal diffusion following the shock which gave values between 25 and 60 per cent in excess of the measured pressure rise. Thus it appears that the subsonic diffusion pressure rise was not achieved, and that the tailpipe pressure rise was well accounted for on the basis of a shock wave alone taking account of measured velocity ratio changes between the throat and tailpipe.

5. CONCLUSIONS

Relations for the conservation of mass and momentum were applied to a bubbly gas–liquid flow to predict the pressure change in variable area flow and the overall pressure rise across a compression shock wave. The flow considered is assumed to undergo isothermal change of

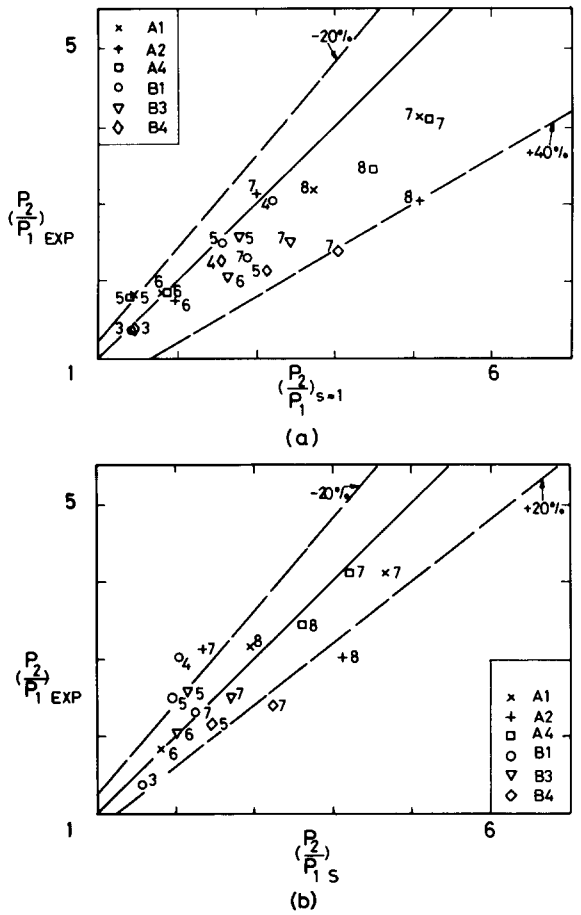

Figure 9. Pressure rise across two-phase shocks: (a) flows assumed to have $S = 1$; (*b*) flows with S accounted for (numbers indicate flow conditions).

pressure and the relative phase velocity term is accounted for. By assuming that the velocity ratio remains constant along the flow path, an expresssion for local pressure as a function of area change could be obtained by direct integration along the pipe length. Static pressure measurements were made in eight venturi configurations for comparison with theoretical prediction. In general, it was shown that in venturis with a sharp contraction three-dimensional flow effects caused appreciable discrepancies in measured wall pressures whilst in venturis with a moderate contraction, the wall pressure in the convergent passage could be predicted with a fair accuracy using the one-dimensional model assuming constant velocity ratio. In supersonic flows in the divergent passage, a steep pressure rise was observed which suggested the presence of a two-phase shock wave. Using values of velocity ratios obtained from void probe measurements, the pressure rise could be predicted to within 20 per cent of the actual values. In recognizing that the scatter in the results was due to the fact that the real shock was not thin and took place in an enlarging passage with additional frictional losses caused by flow separation, it was concluded that the presence of a shock wave gave an acceptable overall description of the pressure rise in the diffuser.

Acknowledgements—The support of the Australian Research Grants Committee and the Australian Institute for Nuclear Science and Engineering is gratefully acknowledged.

REFERENCES

CAMPBELL, I. J. & PITCHER, A. S. 1957 Shock waves in a liquid containing gas bubbles. *Proc. R. Soc. Lond.* **A243**, 534–545.

CAROFANO, G. C. & MCMANUS JR., H. N. 1969 An analytical and experimental study of the flow of air–water and steam–water mixtures in a converging–diverging nozzle. *Proc. Heat Mass Transfer* **2**, 395–417.

DAVIES, A. L. 1967 The speed of sound in mixtures of water and steam. *Proc. EURATOM Sym. Two-phase Flow Dynamics*, Eindhoven.

DAVIS, M. R. 1971 Solutions for two-phase gas–liquid mixture flows without interphase slip or mass transfer. University of New South Wales Rep. 1971/FMT/3.

EDDINGTON, R. B. 1970 Investigation of supersonic phenomena in a two-phase (liquid–gas) tunnel. *AIAA J.* **8**, 65–74.

HENCH, J. E. & JOHNSTON, J. P. 1972 Two-dimensional diffuser performance with subsonic two-phase, air–water flow. *Trans. ASME, J. Basic Engng* **94**, 105–121.

MUIR, J. H. & EICHHORN, R. 1963 Compressible flow of an air–water mixture through a vertical, two-dimensional, converging–diverging nozzle. *Proc.* 1963 *Heat Transfer and Fluid Mechanics Instit.*, pp. 183–204. Stanford University Press, Stanford.

MUIR, J. H. & EICHHORN, R. 1967 Further studies of the compressible flow of an air–water mixture through a vertical, two-dimensional, converging–diverging nozzle. *Proc. JSME* 1967 *Semi-international Symp.*, Tokyo, Vol. 2, pp. 81–91.

SMITH, R. V. 1972 Two-phase, two-component critical flow in a venturi. *Trans. ASME, J. Basic Engng* **94**, 147–155.

TANGREN, R. F., DODGE, C. H. & SEIFERT, H. S. 1949 Compressibility effects in two-phase flows. *J. Appl. Phys.* **20**, 637–645.

THANG, N. T. 1976 A study of two-phase flow through venturis. Ph. D. Thesis, University of New South Wales.

THANG, N. T. & DAVIS, M. R. 1979 The structure of bubbly flow through venturis. *Int. J. Multiphase Flow* **5**, 17–37.

WIJNGAARDEN, L. VAN 1970 On the structure of shock waves in liquid–bubble mixtures. *Appl. Sci. Res.* **22**, 366–381.

WIJNGAARDEN, L. VAN 1972. One-dimensional flow of liquids containing small gas bubbles. *Ann. Rev. Fluid Mech.* **4**, 369–396.

WITTE, J. 1969 Mixing shocks in two-phase flow. *J. Fluid Mech.* **36**, 639–655.